BBC RD 1992/7

Research Department Report

EFFECTS OF WIND TURBINES ON UHF TELEVISION RECEPTION

Field tests in Denmark, November 1991

D.T. Wright, C.Eng., M.I.E.E.

Research Department, Engineering Division
THE BRITISH BROADCASTING CORPORATION

© British Broadcasting Corporation

No part of this publication may be reproduced, stored in a retrieval system, or transmitted in any form or by any means, electronic, mechanical, photocopying, recording, or otherwise, without prior permission.

Published by
BBC Research & Development
Kingswood Warren
Tadworth
Surrey
KT20 6NP
England

http://www.bbc.co.uk/rd

BBC RD 1992/7

EFFECTS OF WIND TURBINES ON UHF TELEVISION RECEPTION: FIELD TESTS IN DENMARK, NOVEMBER 1991

D.T. Wright, C.Eng., M.I.E.E.

Summary

As a result of a planning application for a wind farm comprising 20 wind turbines at Tynewydd Farm, Gifach Goch in Mid Glamorgan, it became necessary to produce a Report discussing any detrimental effects the proposal might have on UHF television reception. In order to make that Report as definitive as possible, it was decided to carry out field tests on the exact model of wind turbine to be used at Tynewydd. This required a field trip to Denmark, and the opportunity was taken to make measurements on two other models of turbine at the same time. This Report presents the analysis of the results for all three turbines.

Index terms: *EMC; wind power; wind turbines; UHF; reception; TV broadcasting; multipath propagation; interference; measurements*

Issued under the Authority of

Ian Childs

Head of Research Department

Research Department, Engineering Division
BRITISH BROADCASTING CORPORATION

1992

EFFECTS OF WIND TURBINES ON UHF TELEVISION RECEPTION: FIELD TESTS IN DENMARK, NOVEMBER 1991

D.T. Wright, C.Eng., M.I.E.E.

1. Introduction 1

2. Methodology 4
   - 2.1 Preliminary method 4
   - 2.2 Direct evaluation of wind turbine characteristics 4

3. Field Measurements 4
   - 3.1 Assessment of interfering signal level 5
   - 3.2 Correction factors 5
   - 3.3 Model calibration factors for NKT 450/37 turbine 7
   - 3.4 Model calibration factors for NKT 300 turbine 8
   - 3.5 Effects of 150 kW turbine 8
   - 3.6 Problems with model calibration techniques 8

4. Direct Analysis of Field Measurement Data 9
   - 4.1 Normalised polar reflection characteristic 9
   - 4.2 Effect of other turbines in the area 9
   - 4.3 Variation of reflection with plane of blades (yaw) 10

5. Other Factors 10
   - 5.1 Effect on normal television broadcasts 10
   - 5.2 Allowance for multiple wind turbines 10

6. Conclusions 10

7. Acknowledgements 12

8. References 13

Appendix 1: Calculation of Normalised Polar Reflection Loss 14

Appendix 2: Spreadsheet Analysis of Field Measurements for Single Nordtank 450 kW Turbine at Langeland 16

Appendix 3: Spreadsheet Analysis of Field Measurements for Various Nordtank 150 kW Turbines at Langeland 19

Appendix 4: Spreadsheet Analysis of Field Measurements for Two Nordtank 300 kW Turbines in Jutland 20

EFFECTS OF WIND TURBINES ON UHF TELEVISION RECEPTION: FIELD TESTS IN DENMARK, NOVEMBER 1991

D.T. Wright, C.Eng., M.I.E.E.

1. INTRODUCTION

The site of any wind farm is likely to be surrounded by a number of UHF television relay stations. These receive signals from a main transmitter and re-transmit them on new channels to communities living in various valleys, where direct reception from the main transmitter is blocked by the hilly or, more often, mountainous terrain. The path to a relay transmitter from its 'parent' is known as a Rebroadcast Link (RBL) path. Fig. 1 shows a typical situation where a wind farm can cause a secondary or ghost image on a television picture. A path difference of 2 km will cause the ghost to be displaced from the main image by one eighth of the width of the television screen. If the ghost is very close to the main image it will, for a given amplitude, be less objectionable. On the other hand, large ghost signals with very small path differences, such as might be caused by actual obstruction of the direct path, can cause loss of colour, buzz on sound, loss of detail in the picture and corruption of Teletext (Ceefax and Oracle) pages. If the wind farm causes any degradation to an RBL signal, it will affect all viewers of the relay and any subsequent down-stream relay transmitters.

For a particular wind farm at Tynewydd in Wales, a preliminary assessment, made in June 1991, highlighted the possibility of interference to the reception of signals from the main transmitter at Wenvoe, at two local relay stations: namely, Blackmill and Ogmore Vale. At that time, it was not possible to predict with sufficient accuracy whether the problem would be serious enough to warrant remedial action. This was mainly due to the lack of available scientific data on the effect of specific wind turbines on UHF television signals.

In order to provide some of the necessary additional information, a field trip was organised to Denmark where there were already many operational wind farms. Two areas were visited. Map 1 shows the first area to the south on the island of Langeland in the area between Dagelokke and Store Snode. Here, there was a single 450 kW turbine of the type planned for use at the site in Wales, with several 150 kW models also available for study in the immediate surrounding area. Map 2 shows the second test area to the north of Jutland, in an area extending from south of Arentsminde toward Birkelse. Here there were a pair of 300 kW turbines in very flat and open surroundings.

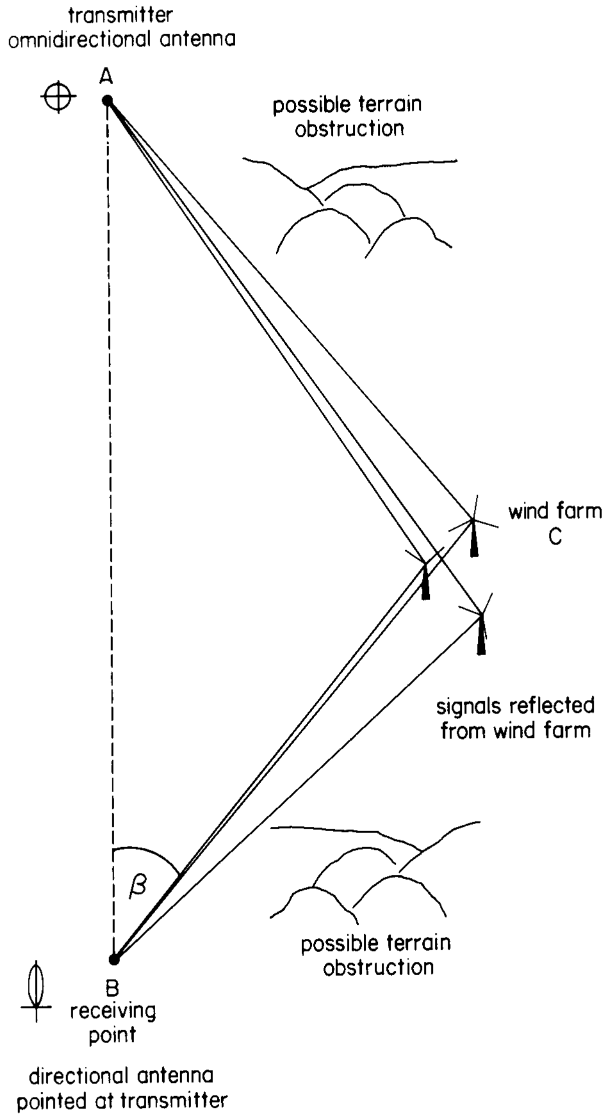
transmitter
omnidirectional antenna
A
possible terrain obstruction
wind farm
C
signals reflected from wind farm
β
possible terrain obstruction
B
receiving point
directional antenna pointed at transmitter

- The problem will be worse if path AB is more obstructed by terrain than paths AC and CB.
- The spacing of the ghost is dependent on the path difference (AC+CB)−AB.

  A path difference of 2 km gives a ghost separation of one eighth of the picture width.
- If β is greater than 60° a standard antenna will normally provide sufficient discrimination against the reflected signals.

  For β between 15° and 60°, a more directional receiving antenna can be used to reduce the level of reflected signals 'seen' by the receiver.

  For β less than 15° even changing to the best available antenna will not help.

Fig. 1 - Ghost signals from a wind farm.

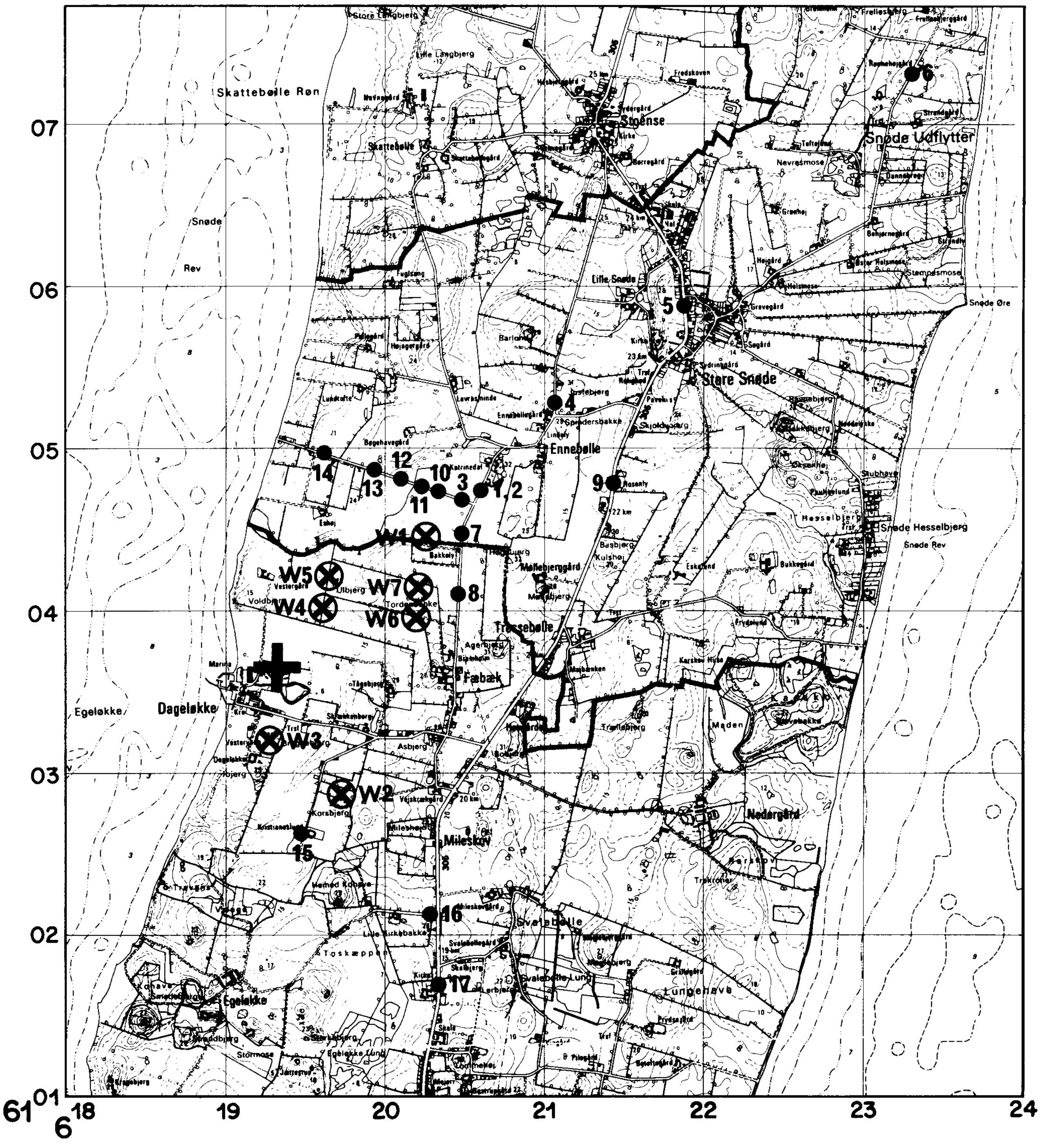

© Copyright Kort- og Matrikelstyrelsen, Denmark (A. 338-92) Part of map: 1412 III SV (Geodætisk Institut)

⊗ Wind turbines under investigation

✚ Test transmitter location

●6 Receiving location with point number

Scale 0 — 1 km

Map 1 - Langeland, Denmark.
Field test area for investigation of 450 kW and 150 kW turbines.

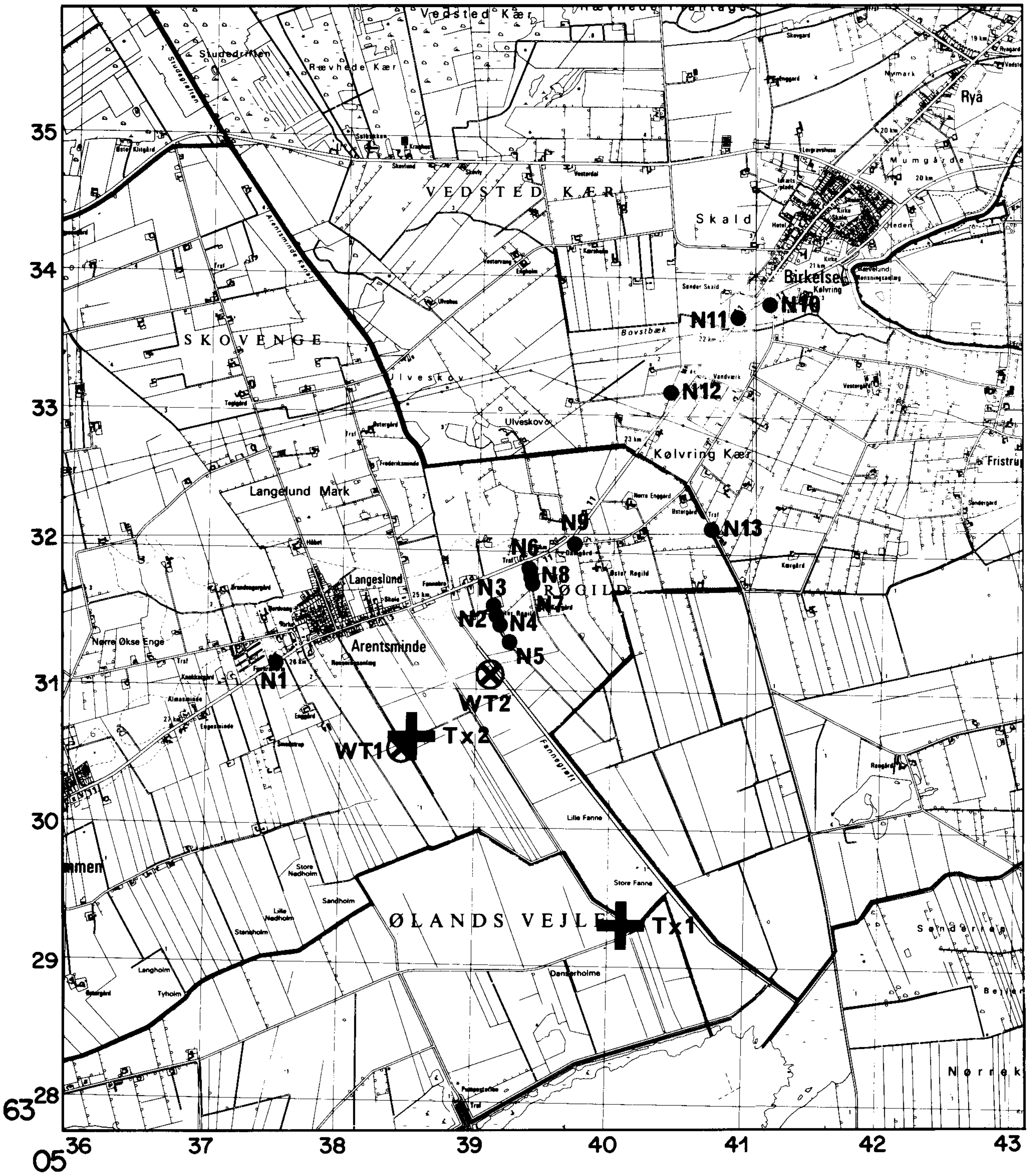

© Copyright Kort- og Matrikelstyrelsen, Denmark (A. 338-92) Part of maps: 1217 II SO, NO, SV, NV (Geodætisk Institut)

⊗ Wind turbines under investigation

✚ Test transmitter location

Scale 0 1 km

● **N12** Receiving location with point number

Map 2 - Han Herred, Denmark.
Field test area for investigation of 300 kW turbines.

All these turbines were manufactured by the Danish company Nordtank and the trip was organised and co-ordinated by Perma Energy who are the UK agents for Nordtank products. The Energy Technology Support Unit (ETSU) of the UK Department of Energy gave some financial support to the project.

The preliminary analysis of some of the actual measurement data for the Danish 450 kW turbine, led to a re-assessment of the situation concerning the two Welsh relay stations, mentioned above; these having been identified as being at possible risk to interference from turbine-induced signal reflections. This Report includes the results of further basic analysis on this turbine, and also on the 150 kW and 300 kW models. In addition, an alternative method of analysis is developed for the presentation of field measurement data in a way which can be compared with existing theoretical models.

2. METHODOLOGY

2.1 Preliminary method

A preliminary method of assessment was used to enable a rapid re-assessment of the situation concerning the proposed wind farm in Wales. This made use of two existing computer modelling algorithms[1, 2] to predict interference levels in situations involving the Nordtank turbines, for which practical measurements had been made during the field tests. These predicted interference levels were then compared with the real-life measurements, in order to obtain figures for the worst case errors between the modelled situations and the real ones. These calibration factors could then be applied to computer-modelled results for various receiving locations around sites in the UK, such as the proposed Tynewydd wind farm. This process of effectively calibrating the wind turbine part of the overall model, to overcome assumed inaccuracies, provided a significant improvement in the accuracy of the modelling process in the one area where the previous lack of data made it unreliable. The overall accuracy of the modelling process should then be much closer to that accepted for planning all other aspects of the UHF television network, where an accuracy of ±5 dB is normally obtained.

Based on the comparison of the two computer-modelling algorithms with practical measurements made in Denmark, the proposed CCIR model described in Ref. 1 was found significantly to overestimate the interference. The linear scatterer model, described in Ref. 2, underestimated by an even greater amount.

2.2 Direct evaluation of wind turbine characteristics

A more direct method of analysing the results is attempted in this Report. Appendix 1 shows that if the geometry of the transmit/receive situation is known, together with the off-axis response characteristics of the transmit and receive antennas, then actual signal-to-interference ratio measurements can be reverse-calculated to place points on a polar diagram. Such a diagram then gives the reflection loss of the wind turbine at a normalised 1 km receiving distance. Identical format polar plots derived from different wind turbines can then easily be compared, either with each other or with plots representing particular modelling algorithms. The main source of error in this type of analysis occurs because it is possible only to estimate the relative level of the interference based upon *chart recorder* measurements (see Section 3.1).

3. FIELD MEASUREMENTS

The field measurements were made by setting up a test transmitter about 1 km from the turbine to be tested, with the transmitting antenna directed toward the turbine. Measurements were made at various distances on the opposite side of the turbine, both in-line and off-centre. The transmissions were made under a special short-term test and development licence kindly provided by the Danish PTT, which allowed transmissions on UHF television channels 29, 38 and 59. The use of three different channels made it possible to identify frequency-dependent effects within any interference mechanism.

Representatives from Nordtank were on hand to stop and start the rotation of the turbine blades as required, or to rotate the mill head (yaw control) to vary or set the plane of rotation of the blades relative to the transmit/receive path.

Due to limitations of time, a continuous yaw variation test was only done for two turbines, namely the 450 kW model and one of the 300 kW models. Also, in each case, only a single receiving location was used during each yaw variation test; this was such that the transmitter, wind turbine and receiver were in line.

For most of the remaining tests, the plane of the blades was set perpendicular to the transmitter-to-wind-turbine path; this having been shown to be the condition which maximised the interference for on-axis measurements.

The weather during the tests was generally dull, with mist or fog affecting visibility for much of the time. As a result, it is likely that the surfaces of the blades of the turbines would have been damp and it should be borne in mind that the effects measured could be affected by the prevailing temperature and humidity conditions (or precipitation).

3.1 Assessment of interfering signal level

To assess the level of the interfering signal, a chart recorder was used to record the amount by which the received field strength fluctuated with the rotation of the turbine blades. Fig. 2 *(overleaf)* shows small samples of a number of different recordings.

It should be noted that there are three cycles of the complex waveform for each revolution of the blade, that is, one for each blade tip. The waveshapes have up to six or twelve points of inflection which suggests that there is an interaction of several interfering components such as from each of the three blades and their interactions with the support tower.

A typical domestic television receiver was used to look for ghosts visible on the picture, and an oscilloscope and trace-recording camera were available to make objective measurements of the relative amplitude of any ghosts which might be seen. It became apparent that, for the particular test locations used, the geometry of the situations gave very small path differences, such that the interference was never manifested as a visible ghost on the picture.

The measured signal level fluctuation can be due to a combination of two effects. At one extreme, the interfering signal could be of constant amplitude but varying in phase relative to the main signal. This would be due to the blade rotation moving the reflection centres and changing the path lengths of the three component interfering signals (presumed as one from each blade). In such a case, the full level of fluctuation will be seen only if the relative phase between the main and interfering signals excurses through both zero and 180° as the blades rotate; this will tend to apply only at short ranges (where the swept area of the blades occupies a significant proportion of the first Fresnel zone). At the other extreme, the level of the interfering signal could be changing, without change in phase relative to the wanted signal; this could be due to the orientation of the metalwork in the blades changing with rotation, and possibly due to the tips of the blades appearing above a terrain obstruction; this will tend to be the case at longer ranges. Most of the fluctuations measured will be a combination of these two effects.

For a constant level of interfering signal, with phase changes in excess of 180°, an interfering signal at a level of $x\%$ relative to the wanted signal would cause the received signal to vary between $(100-x)\%$ and $(100+x)\%$ of the mean value, with the mean value representing the wanted signal level (i.e. the peak-to-peak flutter represents twice the interfering signal). For a varying interference signal at constant relative phase, the maximum flutter will be due to the addition (at 0°) or subtraction (at 180°) of the interference from the wanted signal, with lesser variations at other phase relationships (i.e. the peak-to-peak flutter represents one or less times the interfering signal). For the short ranges used in the test measurements, it is reasonably safe to assume that the varying phase condition applies, and, therefore, to deduce the relative level of the interfering signal from half the peak-to-peak flutter.

In Fig. 2, samples C28, C32 and C84 are examples of the variation of field strength observed with the blades rotating slowly and without significant background effects from other turbines. Samples C36 and C50 are for normal speed rotation (about 36 rpm) where the envelope of the waveform has been modulated by a small amount of background effects from other turbines. The interference level shown in sample C50 was estimated to be −33 dB relative to the wanted signal, and that in sample C36 was −22 dB. Sample C46 has significant background effects which makes it difficult to estimate a value of 'wanted' interference.

3.2 Correction factors

Various corrections need to be applied. The frequency response of the chart recording system was such that, at the normal blade rotation speed of 38 r.p.m., the recorded amplitude of the fluctuations was reduced by about 20%. Each flutter amplitude measurement was, therefore, corrected according to the frequency of the fluctuation (it should be noted that a three-bladed wind turbine produces three cycles of a complex fluctuation waveform for each revolution of the blades). At the Langeland site, where the 450 kW turbine was being measured, there were a lot of background flutter signals due to the presence of several other turbines in the surrounding area; these were easily identified by stopping the blades of the turbine under test. The various fluctuations, which were all at slightly different speeds, can beat together to cause complex patterns lasting tens of seconds (see Fig. 2, sample C50). Fortunately, the effect of adjacent turbines was generally small compared with the effects being measured from the turbine under test; this was mainly achieved by careful choice of the transmit/receive test path relative to other turbines. At the same time, the number of other turbines in the surrounding area at the Langeland test site, limited meaningful off-axis measurements to within an arc extending approximately 45° either side of the axis from the transmitter through the wind turbine. Such off-axis tests would have been

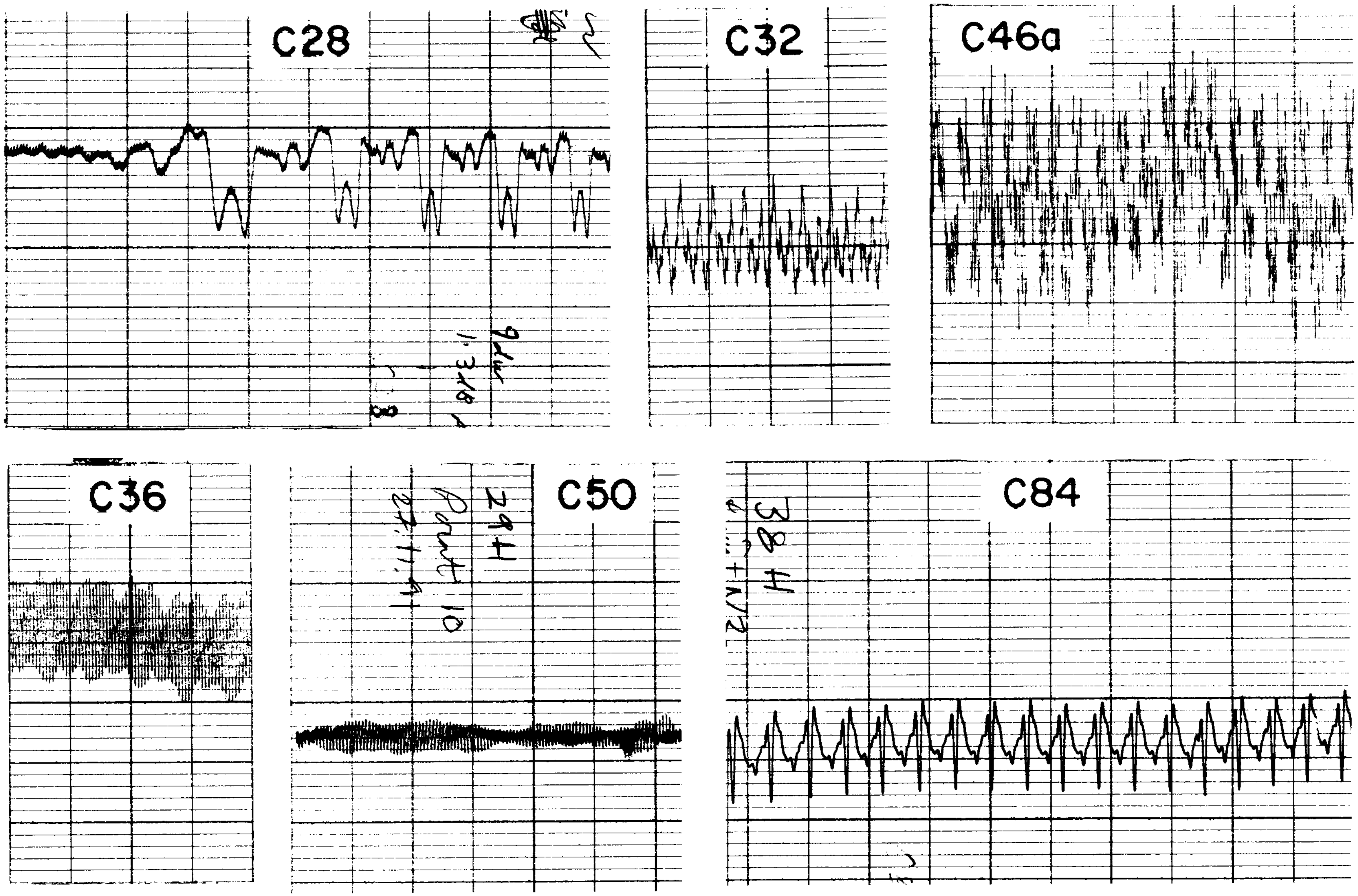

Horizontal scale: 1 cm = 10 secs Vertical scale: 1 cm = 10% chart f.s.d. Offset zero = −78% chart f.s.d.

Fig. 2 - Samples of chart recordings for six different transmit/receive paths and various speeds of blade rotation. They show the variety of signal level patterns which result from the vector additions of the complex of individual signals. They are produced by the ***varying*** *reflections and diffractions from the* ***adjacent*** *turbines, as well as from the principal signal disturbances caused by the turbine directly sited on the transmit/receive path axis.*

NB: C28, C32, C36, C46, C50 and C84 are the chart references as shown in the tables given in Appendices 2 & 4.

relatively easy at the Jutland test site but here, the lack of remaining available time was a limitation.

Depending on the geometry of the transmit and receive locations, corrections may also need to be applied for the directional pattern of the transmit and receive antennas. Furthermore, if any of the three signal paths in the transmitter/receiver/wind turbine triangle (see Fig. 1 and Appendix 1) are not line of sight, then corrections will be required for the consequent diffraction losses. For on-axis reception over flat terrain and relatively short distances, the antenna directivity and terrain corrections are unnecessary. This simplified subset of the measurements was used in the preliminary analysis to produce the Report on the effects likely to be caused by the wind farm in Wales. The only correction applied to those preliminary results, was for the frequency response of the chart recording system. Since then, it has been possible to include a correction for terrain losses which occurred on the transmitter-to-receiver path at two of the test points; these are taken into account in the results presented in Tables 1 and 2, which show comparisons of signal-to-interference ratios as estimated from the chart recordings, with the values predicted by the two modelling algorithms.

3.3 Model calibration factors for NKT 450/37 turbine

Table 1 shows the comparison for the NKT 450/37 turbine. The test locations listed here were all on-axis, and the input parameters to the modelling algorithm were arbitrarily fixed at 100 m^2 for blade area and 17 m for blade length. The model software then evaluates the blade width as 5.9 metres. Due to lack of information available from the manufacturer, and the complex shape of the blades, it is difficult to estimate the actual blade area.

It can be seen, that the model was found to overestimate the interference level when using the proposed CCIR modelling algorithm[1], which is believed to assume reflection from *two* blades, possibly made of metal. The overestimate was at least 17.4 dB (a factor of 7.4 times). The magnitude of this overestimate is to be expected, since the blades of the real turbine are constructed mainly from fibreglass rather than metal. Another modelling algorithm, proposed by Tegth[2], which assumes the interference is generated by a wire running the entire length of *two* blades (the turbines tested had three blades), underestimated the level of interference by up to 19 dB for the NKT 450/37 turbine; that is, the practical level of interference can be up to 8.9 times that predicted by the model. One possible explanation for this is that the metal components inside the blade are far more efficient at re-radiating energy than would be expected from a straight wire. Alternatively, the fibreglass could have been behaving as semi-transparent metal. A higher level of interference observed on UHF channel 29, relative to channels 38 and 59, suggests that the enhancement is more likely to be due to a tuning effect within the metalwork, rather than reflection from the fibreglass. The only way to resolve this uncertainty is to test a wind turbine with no metal in the blades; if it is the fibreglass which is causing the effect, the results will be similar.

Table 1: On-axis measurements MKT 450/37

Test point		Model reference	Wanted/interference field strength ratio (dB)				Correction factor for model (dB)
No.	Range from wind turbine		Model (flat terrain)	Terrain correction	Terrain corrected model	Worst measured	
3	0.32 km	CCIR [1]	2.6	0	2.6	20	−17.4
4	1.14 km	"	− 2.7	0	− 2.7	27	−29.7
5	1.85 km	"	3.9	−8.3	− 4.4	23	−27.4
6	4.10 km	"	4.6	−7.2	− 2.6	20	−22.6
3	0.32 km	Tegth [2]	39.0	0	39.0	20	+19.0
4	1.14 km	"	33.7	0	33.7	27	+ 6.7
5	1.85 km	"	40.3	−8.3	32.0	23	+ 9.0
6	4.10 km	"	41.0	−7.2	33.8	20	+13.8

Transmitter to wind turbine distance		1.21 km
Transmitter antenna height		17 m
Receiving antenna height		10 m
Model input parameters:	blade area	100 m^2
	blade length	17 m
	wind turbine height	50 m

3.4 Model calibration factors for NKT 300 turbine

Table 2 shows a similar analysis for tests carried out on the 300 kW turbine. For this turbine, it can be seen that the proposed CCIR model gave an overestimate of at least 14 dB, and the Tegth linear scatterer algorithm gave an underestimate of up to 21.1 dB.

In the case of the 300 kW turbine, the enhancement of interference occurred on channel 59 rather than 29. This increase in resonant frequency for a reduction in turbine dimensions is not, however, consistent with the change in physical size; the frequency increases by 1.4 times while the blade length reduces by a factor of only 1.2.

3.5 Effects of 150 kW turbine

The levels of interference, from the various 150 kW turbines in the area surrounding the 450 kW model at Langeland, were noted to be generally at less than −30 dB relative to the wanted signal. There was no obvious enhancement on any of the three UHF channels used for the tests. The model calibration exercise has not been undertaken for this type of turbine.

3.6 Problems with model calibration techniques

The accuracy of the computer modelling technique is limited by the use of a six figure grid reference which gives 100 m resolution of northings and eastings. This quantisation causes significant errors with the small dimensions involved. For test locations which are known to be on the transmitter/wind turbine axis, results can appear up to two or more degrees off axis, with a consequent change in the predicted ratio of wanted-to-interfering field. For on-axis measurements, it is possible to eliminate the angular component of the quantisation error by rotating the transmit receive axis to fit along a horizontal or vertical grid line. However, this still leaves distances quantised to the nearest 100 m. This effect can be seen in Table 2 where the identical model predictions occur for different receiving distances. The existence of quantisation problems flagged the need for a better and more direct way of dealing with the relatively short transmit/receive paths used in the tests.

Table 2: On-axis measurements MKT 300

Test point		Model reference	Wanted/interference field strength ratio (dB)				Correction factor for model (dB)
No.	Range from wind turbine		Model (flat terrain)	Terrain correction	Terrain corrected model	Worst measured	
N2	0.59 km	CCIR[1]	3.7	-		19	−15.3
N3	0.63 km	"	3.7	-		25	−21.3
N6	1.03 km	"	5.5	-		27	−21.5
N8	0.99 km	"	5.5	9.0	− 3.5	12	−15.5
N10	3.61 km	"	0.7	-		28	−27.3
N11	3.39 km	"	1.4	-		22	−20.6
N12	2.67 km	"	2.0	-		25	−23.0
N2	0.59 km	Tegth[2]	40.1	-		19	+21.1
N3	0.63 km	"	40.1	-		25	+15.1
N6	1.03 km	"	41.8	-		27	+14.8
N8	0.99 km	"	41.8	9.0	32.8	12	+20.8
N10	3.61 km	"	37.1	-		28	+ 9.1
N11	3.39 km	"	37.8	-		22	+15.8
N12	2.67 km	"	38.4	-		25	+13.4

Transmitter to wind turbine distance		0.53 km
Transmitter antenna height		17 m
Receiving antenna height		10 m
Model input parameters:	blade area	100 m^2
	blade length	17 m
	wind turbine height	50 m

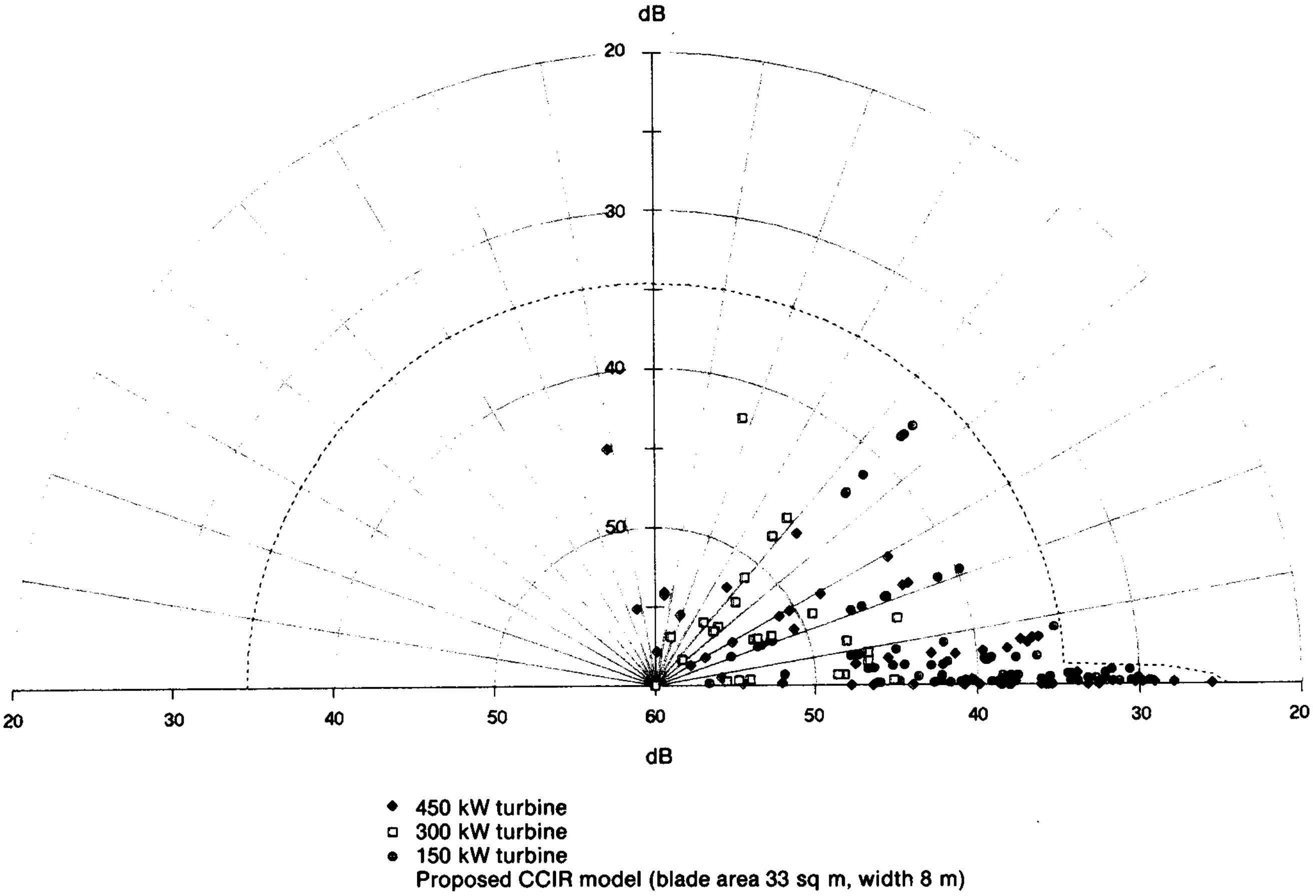

Fig. 3 - Normalised polar reflection loss.

4. DIRECT ANALYSIS OF FIELD MEASUREMENT DATA

4.1 Normalised polar reflection characteristic

Appendix 1 discusses the theory which relates the signal-to-interference ratio at a receiving point to the normalised polar reflection loss of a wind turbine. The limited results which are available have all been placed on the single chart which appears in Fig. 3. This chart is a polar plot of values of $k\theta$ against θ; each measurement recorded produces a separate point; most test locations give rise to several points relating to different channels and polarisations. Edited versions of the spreadsheet, used to collate the data for Fig. 3, appear in Appendices 2, 3 and 4.

By selecting points which appear on the chart according to wind turbine type, television channel or distance from the turbine, it should be possible to determine areas where there is a correlation between points, and to identify points where errors may have occurred. For example, points which do not fit a particular trend may have some common factor, such as short range from the transmitter, which indicates that they may be better grouped under a separate category. For the relatively small number of measurements taken in Denmark, however, it will be difficult to be conclusive in such respects; the number of results in some sub-categories will be too small to indicate trends.

In Fig. 3, the lack of a forward lobe effect for the 150 kW turbine (yellow markers) should be noted. It is possible that there may be a correlation between the presence of a forward lobe and the presence of enhanced interference levels at particular frequencies.

A curve has been added to Fig. 3 which shows a best-fit characteristic according to the proposed CCIR modelling algorithm[1]; the input parameters for this curve, which were arrived at on a trial and error basis, specify a blade area of 33 m^2 and a blade width of 8 metres. The actual blade was tapered with a mean width of about 1.4 metres.

4.2 Effect of other turbines in the area

In the early stages of the normalised polar reflection analysis, there appeared to be a considerably enhanced response for some of the 450 kW turbine measurements taken at locations more than 70° off axis. It was subsequently decided that, for all measurements of this turbine more than 50° off axis, with the receiving antenna pointing toward the transmitter, it was more likely that the measurement related to one of the various 150 kW turbines in the surrounding area which happened to be almost across the direct transmit/receive path. As a result, all the significantly off-axis measurements for the 450 kW turbine, where the toward-transmitter receive antenna bearing was actually directed in the general direction of a 150 kW turbine, have been re-designated as measurements of a 150 kW turbine. Other measurements which were taken at such points, with the receive antenna pointing toward the 450 kW turbine, should show only a secondary effect from the presence of this other source of interference, and these have, therefore, been left in the 450 kW section of the analysis.

4.3 Variation of reflection with plane of blades (yaw)

At one on-axis test location for each of the 450 kW and 300 kW turbines, the mill head was turned to see how the interference level changed with the plane of the blades. In general terms, the interference was at maximum when the plane of the blades was perpendicular to the transmit/receive path, and a minimum when parallel to it. On the basis that the response could be proportional to the product of the projected areas of the blades along the transmit path and the receive path, one might expect the response to be proportional to $\cos^2(\phi)$. On the other hand, the response could be proportional to the area of the blades projected across the path which passes through the turbine; in this case the response would be proportional to $\cos(\phi)$. Fig. 4 shows the chart recordings for each turbine during the yaw variation test. From these it can be seen that the response at 45° (aproximately halfway between the 'Perpendicular' and 'In-line' positions shown in Fig. 4) lies between about 55% and 65% of the maximum; this suggests that the variation is proportional to $\cos^{1.3}(\phi)$ rather than either $\cos(\phi)$ or $\cos^2(\phi)$. Further tests are needed in order to give a more definitive figure, and explanation, for the exponent.

5. OTHER FACTORS

5.1 Effect on normal television broadcasts

At some locations, the quality of normal television broadcasts received 'through' or 'around' wind turbines and wind farms was assessed. There were no realistic receiving situations where any subjective picture degradation occurred, even though it was possible to record signal level fluctuations which indicated the presence of an interfering signal at a relative level of −27 dB. In such situations, however, the turbines in question were generally the smaller 150 kW models which were shown by the measurements to cause effects at UHF frequencies which were at least 10 dB lower than either the 300 kW or 450 kW models.

5.2 Allowance for multiple wind turbines

A correction factor for multiple turbines will need to be applied to any modelling results for a single wind turbine. Although unlikely, the worst case situation is when the interfering signals from all turbines have the same delay but have their carrier waves in random phase. In such a case, the overall interference level would be determined by the power sum of all the sources. For twenty turbines this would be 13 dB greater than that for a single turbine, and for 100 turbines the figure would be 20 dB. If each individual reflection is below the threshold of visibility and the delays are such that the reflections do not overlap each other, then it could be argued that the combined effect will remain below the threshold of visibility. On the other hand, it seems inconceivable that 100 sub-threshold interfering signals could fail to have some effect on the picture, even if only to worsen the subjective noise level. It is thought that, in a practical situation involving 20 turbines, the interference will probably increase by about half the amount in decibels which would be expected from the power sum — say 8 dB for 20 turbines and 12 dB for 100 turbines. As there is no practical evidence to support either figure, it is prudent to assume the higher one, since the difference is of the same order as other modelling errors.

6. CONCLUSIONS

Although the tests conducted in Denmark were very limited, they have provided useful information, enabling a conclusion to be drawn concerning the question of whether the proposed wind farm in Wales would affect UHF television reception at two local relay stations. It has also been possible to develop a method of analysing and presenting measurement results which can be used for the assessment of future turbines. Applying this method to the results obtained in Denmark has produced a combined polar plot sufficient to indicate inaccuracies in existing modelling algorithms. It is to be hoped that, eventually, it will be possible to produce a polar plot of normalised polar reflection loss for every type of turbine likely to be used in the UK. These can then be used to enhance the accuracy of future computer modelling methods.

Evidence obtained to date suggests that the

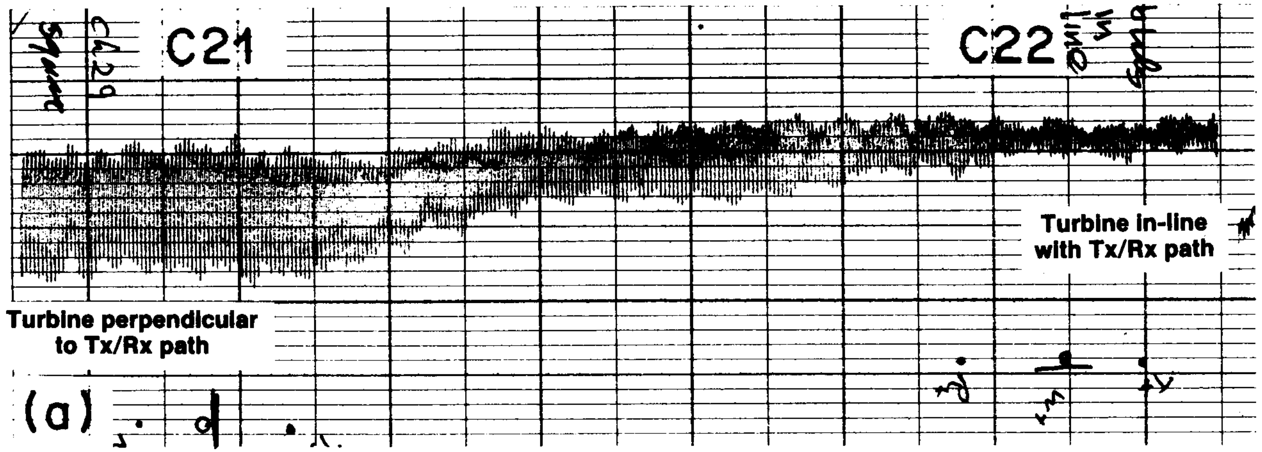

(a) 450 kW (Langeland)

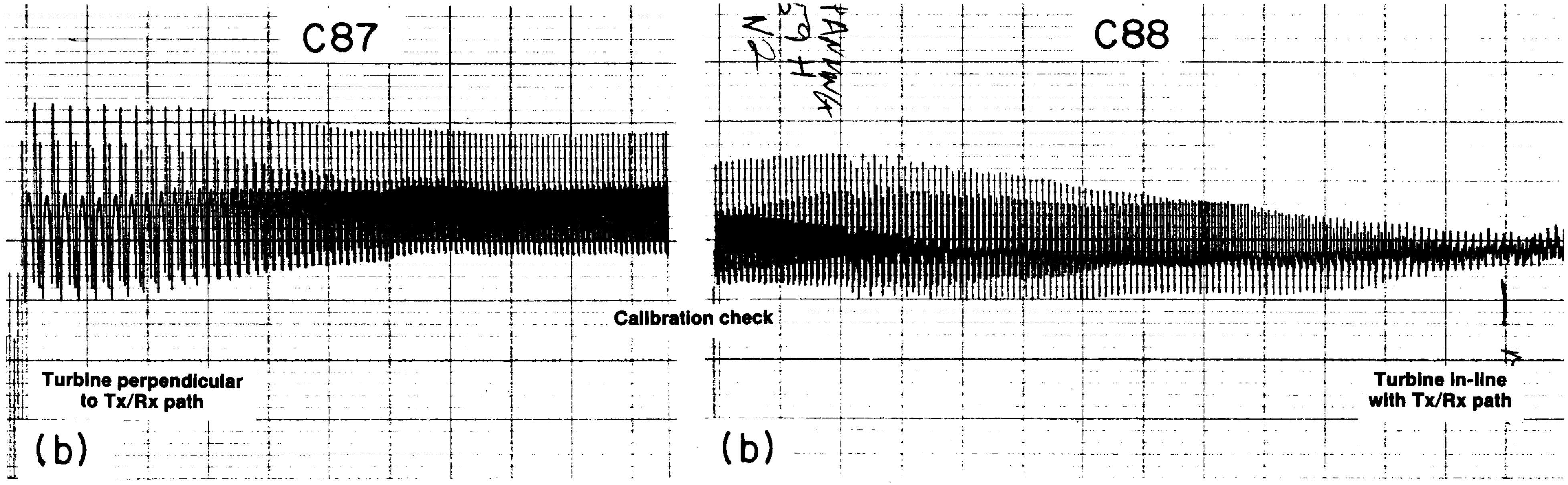

(b) 300 kW (Jutland)

Horizontal scale: 1 cm = 10 secs Vertical scale: 1 cm = 10% chart f.s.d. Offset zero = −78% chart f.s.d.

Fig. 4 - Chart recordings made while the plane of the turbine blade rotation was yawed through 90° from a position perpendicular to the transmitter/receiver path, to an in-line position.

NB: C21, C22, C87 and C88 are the chart references as shown in the tables given in Appendices 2 & 4.

proposed CCIR model for the interference from a wind turbine is pessimistic, in that it overestimates the level of interference by at least 10 dB with an arbitrarily chosen blade area of 100 m^2. Reducing the blade area parameter of the model will reduce the correction factor, but this will also make the re-radiation polar diagram more omnidirectional due to the evaluated blade width also being reduced. It should be noted that, using the current formula, the actual blade width gives a polar response with a front lobe that is rather too wide. Any future model should have a facility for direct input of two parameters, namely, maximum re-radiation level and forward lobe beam width. Only where direct values for these are not available, should appropriate formulae be used to evaluate approximate (pessimistic) values from the physical dimensions of the turbine blades, the number of blades and the material used for the blades.

The linear scatterer model is not considered appropriate to the types of turbine measured. Whilst, in theoretical terms, it would seem to represent best the known metal content within the blades of the Nordtank turbines, it grossly underestimates the level of interference without obvious reason *vis-à-vis* the input parameters. Furthermore, it seems to produce large changes in predicted interference for small changes of angle close to the on-axis situation. Such variations are not consistent with the broader polar responses indicated from the field measurements. As a result, it is considered that the Tegth model could be dangerously optimistic about slightly off-axis situations, even after calibration correction.

For the two wind turbine models tested in some detail, it was observed that the level of re-radiation is frequency dependent, giving enhancements on different channels for different turbines. Limited measurements on 150 kW turbines showed no obvious enhancement of interference amongst the three UHF channels used for the tests. It is, of course, possible that such an enhancement exists at a frequency beyond the top of the UHF broadcast band. The mechanism for the frequency dependence has yet to be explained. Further work is planned to investigate the elctromagnetic properties of a section of wind turbine blade to determine whether the transparency to radio frequencies is impaired by dirt and/or dampness or at particular frequencies.

The Nordtank 150 kW turbine appears to produce levels of interference at least 10 dB lower than the 300 kW or 450 kW models. On this basis, it should have negligible effect on UHF television transmissions. The lower levels of measured interference may be due to the fact that the 150 kW turbine did not have any obvious enhancement of interference level on any of the UHF channels used for the tests. An enhancement may exist at some other frequency but this is thought likely to be above the top of the UHF band. It may be that, for the 150 kW turbine, the absence of both an enhancement and a forward lobe are related.

Observations of normal television broadcasts made during the tests failed to discover any situation where the television was impaired to an extent which could be attributed to a wind farm. It must be noted, however, that most of the turbines on such wind farms were of the smaller 150 kW size which was noted to cause considerably less effect at UHF than either the 300 kW or 450 kW models. It should also be noted that in the United Kingdom, which is relatively hilly compared with Denmark, the interference level at a receiving location can be enhanced considerably. This is due to terrain obstruction of the wanted signal path whilst the two hops of the interfering signal path remain unobstructed.

It cannot be ruled out that the close range of the site test transmitter to the wind turbine under test, may have enhanced the observed levels of reflection. Under such conditions, the sweep of the turbine blades occupies a substantial proportion of the first Fresnel zone. But it would be unsafe to assume that this is the case, until further work has been done to explain any such mechanism.

Further work also needs to be done to establish a valid method for assessing the combined effects of many wind turbines. This is unlikely to be achievable in the immediate future due to a combination of limited resources for field investigation work and the current lack, within the UK, of a diversity of operational wind farms on which such studies could be based.

7. ACKNOWLEDGEMENTS

The BBC is grateful to the organisations within the wind turbine circle, and other organisations in Denmark, without whose co-operation and assistance these tests could not have been made. These include: Nordtank, who provided operators to control the turbines; Perma Energy, the UK agent for Nordtank, who co-ordinated the visit; L.M. Glasfiber, who provided details of the construction of the blades; the National Telecom Agency Denmark, who provided a special test transmission licence; Telecom A/S, the Danish transmission authority; and the Energy Technology Support Unit of the UK Department of Energy, who have agreed to contribute towards the costs of the project.

8. REFERENCES

1. EBU, 1990. Report of first meeting of EBU Ad-hoc Group R2/WRO. European Broadcasting Union GT R2 376, Appendix 1, August 1990.

2. TEGTH, U., 1990. TV interference measurements at Kalkugnen test windmill. *TELE* (English edition), **32**, No. 2, 1980, pp 45-53 (Linear scatterer).

APPENDIX 1

Calculation of Normalised Polar Reflection Loss

This Appendix derives the formula for the relative level of interfering signal at a receiving location. This formula is then transposed so that it can be used to give polar coordinates for the reflectivity of the turbine toward a receiving point. The required inputs to the resulting formula are: the estimated relative level of interfering signal at the test point; the geometry details of the transmit/receive paths; and the off-axis response characteristics of the transmit and receive antennas.

T W and R	represent respectively the transmitter, wind turbine and receiver as illustrated in Fig. A1.1 below.
$\mathbf{d}_{TR}$	is the distance, in km, from the transmitter to the receiver.
$\mathbf{d}_{TW}$	is the distance, in km, from the transmitter to the wind turbine.
$\mathbf{d}_{WR}$	is the distance, in km, from the wind turbine to the receiver.
α	is the angle by which the receiver is off the axis of the transmit antenna, which is directed toward the wind turbine.
β	is the angle by which the wind turbine is off the axis of the receive antenna which is normally directed toward the transmitter.
θ	is the angle which the receiver subtends from the wind turbine relative to axis from T to W.
$P(\alpha)$	is the function describing the off-axis reduction in gain of the transmit antenna in the horizontal plane. Expressed in dB, values for various angles will be zero or positive.
$Q(\beta)$	is the function describing the loss of response of the receive antenna to off-axis signals. Expressed in dB, values for various angles will be zero or positive.
$k(\theta)$	is a function which describes, in terms of polar response, the ratio of the field strength incoming to the wind turbine relative to the reflected signal measured at a distance of 1 km from the turbine. This can be referred as the **normalised polar reflection loss** which can be expressed in dB.

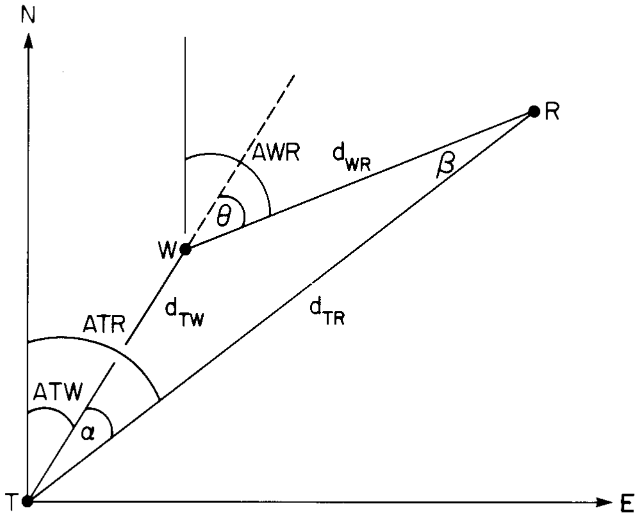

Fig. A1.1 - Relative disposition of transmitter receiver and wind turbine.

If the effective radiated power of the transmitter is EdBW

Then the wanted field strength at the receiver will be given by:

$$FS_{\text{wanted}} = E - P(\alpha) + 77 - 20\log_{10}\mathbf{d}_{\text{TR}} \quad \text{dB}\mu\text{V/m} \tag{1}$$

The field strength at the wind turbine will be:

$$FS_{\text{turbine}} = E + 77 - 20\log_{10}\mathbf{d}_{\text{TW}} \quad \text{dB}\mu\text{V/m} \tag{2}$$

The field strength of the resulting field at a distance of 1 km from the wind turbine will be:

$$FS_{\text{reflected 1 km}} = FS_{\text{turbine}} - k(\theta) \quad \text{dB}\mu\text{V/m}$$

At the actual receiver distance from the wind turbine this becomes:

$$FS_{\text{interfering}} = FS_{\text{turbine}} - k(\theta) - 20\log_{10}\mathbf{d}_{\text{WR}} \quad \text{dB}\mu\text{V/m} \tag{3}$$

The directivity of the receiving antenna further reduces the effective level of the interfering signal by $Q(\beta)$ dB so that the ratio of the wanted to interfering signal levels at the output of the receiving antenna down-lead will be given by:

$$SI\text{ratio} = \text{eqn}(1) - \text{eqn}(3) + Q(\beta) \qquad \text{dB}$$

which reduces to:

$$SI\text{ratio} = k(\theta) + Q(\beta) - P(\alpha) + 20\log_{10}((\mathbf{d}_{\text{TW}} * \mathbf{d}_{\text{WR}}) / \mathbf{d}_{\text{TR}}) \qquad \text{dB}$$

This can be transposed to give:

$$k(\theta) = SI\text{ratio} + P(\alpha) - Q(\beta) - 20\log_{10}((\mathbf{d}_{\text{TW}} * \mathbf{d}_{\text{WR}}) / \mathbf{d}_{\text{TR}}) \qquad \text{dB}$$

For test situations, where the receiving antenna is pointed toward the wind turbine rather than the transmitter, the sign of the $Q(\beta)$ component should be changed to convert the rejection factor for the unwanted signal into the appropriate enhancement.

Correction for diffraction loss effects

The above formula ignores the effects of diffraction losses on the constituent paths. For situations where one or more of the paths is not line of sight, the diffraction losses need to be estimated from terrain profile information. The signal to interference ratio estimated from field measurements can then be corrected to the value it would have been if the diffraction loss did not exist, before applying the above formula.

APPENDIX 2

Spreadsheet Analysis of Field Measurements for Single Nordtank 450 kW Turbine at Langeland

Test locn	Chart ref.	Tx grid E	Tx grid N	W T grid E	W T grid N	Rx grid E	Rx grid N	Dist.T-W (km)	Dist.T-R (km)	Dist.W-R (km)	α (deg)	$P(\alpha)$ (dB)	β (deg)	$Q(\beta)$ (dB)	Chan	Pol.	p−p max 2% divs	cycles in 10 s	F strength (dbμV/m)	Diffraction loss (dB)	S/I max (dB)	$K(\theta)$ (dB)	θ (degrees)	Comments
1	C1	19350	3660	20250	4480	20590	4730	1.22	1.64	0.42	2	0.01	4	0.10	29	H	3.00	17			31	41	6	
1	C2	19350	3660	20250	4480	20590	4730	1.22	1.64	0.42	2	0.01	4	0.10	38	H	1.40	19			37	47	6	
1	C3	19350	3660	20250	4480	20590	4730	1.22	1.64	0.42	2	0.01	4	0.10	59	H	5.40	3.3			28	38	6	
1	C4	19350	3660	20250	4480	20590	4730	1.22	1.64	0.42	2	0.01	4	0.10	29	H	3.10	18			30	40	6	
1	C5	19350	3660	20250	4480	20590	4730	1.22	1.64	0.42	2	0.01	4	0.10	50	H	5.00	3.3			28	38	6	
1A	C6	19350	3660	20250	4480	20620	4805	1.22	1.71	0.49	0	0.00	1	0.00	59	H	0.70	19			45	54	1	
1A	C7	19350	3660	20250	4480	20620	4805	1.22	1.71	0.49	0	0.00	1	0.00	38	H	0.80	18			43	52	1	
1A	C8	19350	3660	20250	4480	20620	4805	1.22	1.71	0.49	0	0.00	1	0.00	29	H	2.90	17			31	40	1	
1B	C9	19350	3660	20250	4480	20570	4710	1.22	1.61	0.39	2	0.01	5	0.13	29	H	6.00	18			26	37	7	
1B	C10	19350	3660	20250	4480	20570	4710	1.22	1.61	0.39	2	0.01	5	0.13	38	H	0.60	18			45	56	7	
1B	C11	19350	3660	20250	4480	20570	4710	1.22	1.61	0.39	2	0.01	5	0.13	59	H	2.00	18			35	45	7	
1B	C11A	19350	3660	20250	4480	20570	4710	1.22	1.61	0.39	2	0.01	5	0.13	59	H	2.80	18			32	43	7	
2A	C12	19350	3660	20250	4480	20510	4575	1.22	1.48	0.28	4	0.08	18	1.69	59	H	1.20	18			39	51	22	
2A	C13	19350	3660	20250	4480	20510	4575	1.22	1.48	0.28	4	0.08	18	1.69	38	H	2.80	18			32	43	22	
2A	C14	19350	3660	20250	4480	20510	4575	1.22	1.48	0.28	4	0.08	18	1.69	29	H	2.50	18			32	43	22	
2B	C15	19350	3660	20250	4480	19980	4845	1.22	1.34	0.45	−20	1.98	−64	−25.00	29	H	12.00	18			20	54	84	Toward turbine
2B	C16	19350	3660	20250	4480	19980	4845	1.22	1.34	0.45	−20	1.98	−64	−25.00	38	H	3.50	20			29	64	84	Toward turbine
2B	C17	19350	3660	20250	4480	19980	4845	1.22	1.34	0.45	−20	1.98	−64	−25.00	59	H	12.00	18			19	54	84	Toward turbine
3	C17A	19350	3660	20250	4480	20480	4690	1.22	1.53	0.31	0	0.00	0	0.00	29	H	4.60	17			28	40	0	
3	C18	19350	3660	20250	4480	20480	4690	1.22	1.53	0.31	0	0.00	0	0.00	29	H	8.40	18			23	36	0	
3	C19	19350	3660	20250	4480	20480	4690	1.22	1.53	0.31	0	0.00	0	0.00	29	H	3.10	18			32	44	0	
3	C20	19350	3660	20250	4480	20480	4690	1.22	1.53	0.31	0	0.00	0	0.00	29	H	3.90	17			29	41	0	
3	C21	19350	3660	20250	4480	20480	4690	1.22	1.53	0.31	0	0.00	0	0.00	29	H	8.10	18			24	36	0	
3	C22	19350	3660	20250	4480	20480	4690	1.22	1.53	0.31	0	0.00	0	0.00	29	H	2.20	18			36	48	0	
3	C23	19350	3660	20250	4480	20480	4690	1.22	1.53	0.31	0	0.00	0	0.00	29	H	14.50	1.25			20	32	0	
3	C24	19350	3660	20250	4480	20480	4690	1.22	1.53	0.31	0	0.00	0	0.00	29	H	7.80	2.5			26	38	0	
3	C25	19350	3660	20250	4480	20480	4690	1.22	1.53	0.31	0	0.00	0	0.00	29	H	3.00	8.5			34	46	0	
3	C26	19350	3660	20250	4480	20480	4690	1.22	1.53	0.31	0	0.00	0	0.00	29	H	8.00	6.5			26	38	0	
3	C27	19350	3660	20250	4480	20480	4690	1.22	1.53	0.31	0	0.00	0	0.00	29	H	4.60	17			26	39	0	
3	C28	19350	3660	20250	4480	20480	4690	1.22	1.53	0.31	0	0.00	0	0.00	29	H	8.50	1.3			24	36	0	
4	C29	19350	3660	20250	4480	21070	5270	1.22	2.36	1.14	−1	0.00	−1	0.00	29	H	4.70	18	72.8	1.7	28	34	2	
5	C30	19350	3660	20250	4480	21450	5890	1.22	3.06	1.85	−4	0.10	−3	0.04	29	H	6.70	8.6	57.9	8.3	26	37	7	
5	C31	19350	3660	20250	4480	21450	5890	1.22	3.06	1.85	−4	0.10	−3	0.04	29	H	7.60	1	57.9	8.3	25	36	7	
5	C32	19350	3660	20250	4480	21450	5890	1.22	3.06	1.85	−4	0.10	−3	0.04	29	H	8.00	3.2	57.9	8.3	25	36	7	
6	C33	19350	3660	20250	4480	23270	7260	1.22	5.32	4.10	0	0.00	0	0.00	29	H	8.80	18	57	7.2	23	30	0	
6	C34	19350	3660	20250	4480	23270	7260	1.22	5.32	4.10	0	0.00	0	0.00	29	H	11.70	6	57	7.2	21	29	0	
6	C35	19350	3660	20250	4480	23270	7260	1.22	5.32	4.10	0	0.00	0	0.00	29	H	13.00	2.5	57	7.2	20	28	0	
6	C36	19350	3660	20250	4480	23270	7260	1.22	5.32	4.10	0	0.00	0	0.00	29	H	9.00	15	57	7.2	22	30	0	
7	C37	19350	3660	20250	4480	20480	4460	1.22	1.38	0.23	7	0.25	40	8.93		H	1.20	18	76.6	2.7	39	47	47	
7	C38	19350	3660	20250	4480	20480	4460	1.22	1.38	0.23	7	0.25	40	− 8.93		H	0.80	18		2.7	42	68	47	Toward turbine

Appendix 2 *(cont.)*

Test locn	Chart ref.	Tx grid E	Tx grid N	W T grid E	W T grid N	Rx grid E	Rx grid N	Dist.T-W (km)	Dist.T-R (km)	Dist.W-R (km)	α (deg)	$P(\alpha)$ (dB)	β (deg)	$Q(\beta)$ (dB)	Chan	Pol.	p–p max 2% divs	cycles in 10 s	F strength (dbμV/m)	Diffraction loss (dB)	S/I max (dB)	$K(\theta)$ (dB)	θ (degrees)	Comments
8	C39	19350	3660	20250	4480	20470	4120	1.22	1.21	0.42	20	1.08	81	−25.00			29.00	18			11	45	101	
3	C42	19350	3660	20250	4480	20480	4690	1.22	1.53	0.31	0	0.00	0	0.00	29	H	5.30	18			26	38	0	
3	C43	19350	3660	20250	4480	20480	4690	1.22	1.53	0.31	0	0.00	0	0.00	29	V	3.70	17			29	41	0	
3	C44	19350	3660	20250	4480	20480	4690	1.22	1.53	0.31	0	0.00	0	0.00	29	H	5.20	17			26	38	0	
3	C45	19350	3660	20250	4480	20480	4690	1.22	1.53	0.31	0	0.00	0	0.00	29	V	10.00	14			21	33	0	
3	C46	19350	3660	20250	4480	20480	4690	1.22	1.53	0.31	0	0.00	0	0.00	29	V	8.20	1.6			23	35	0	
3	C47	19350	3660	20250	4480	20480	4690	1.22	1.53	0.31	0	0.00	0	0.00	29	H	14.00	18			13	26	0	
9		19350	3660	20250	4480	21440	4790	1.22	2.38	1.23	14	0.52	14	0.51			0.10		56.5	18	62	84	28	
10	C50	19350	3660	20250	4480	20330	4720	1.22	1.44	0.25	−5	0.12	−24	3.07	29	H	2.50	·18	77		33	43	29	
10	C51	19350	3660	20250	4480	20330	4720	1.22	1.44	0.25	−5	0.06	−24	1.61	29	V	1.70	17	76		36	48	29	
10	C52	19350	3660	20250	4480	20330	4720	1.22	1.44	0.25	−5	0.06	−24	1.61	38	V	0.80	18	77		43	54	29	
10	C53	19350	3660	20250	4480	20330	4720	1.22	1.44	0.25	−5	0.12	−24	3.07	38	H	1.10	18	78		40	50	29	
10	C54	19350	3660	20250	4480	20330	4720	1.22	1.44	0.25	−5	0.12	−24	3.07	59	H	0.50	18	76		47	57	29	
10	C55	19350	3660	20250	4480	20330	4720	1.22	1.44	0.25	−5	0.06	−24	1.61	59	V	0.70	18	76		45	56	29	
10	C56	19350	3660	20250	4480	20330	4720	1.22	1.44	0.25	−5	0.12	−24	−3.07	29	H	2.00	19	76		34	51	29	Toward turbine
11	C58	19350	3660	20250	4480	20220	4750	1.22	1.39	0.27	−9	0.42	−45	−4.00	29	H	1.80	19	74		35	52	54	To gen. meas. $Q(\beta)$
12	C60	19350	3660	20250	4480	20120	4790	1.22	1.37	0.34	−13	0.91	−57	−8.00	29	H	1.70	20	67		36	55	70	To gen. meas. $Q(\beta)$
13	C62	19350	3660	20250	4480	19950	4850	1.22	1.33	0.48	−21	2.25	−66	−13.00	29	H	2.70	20	65	3.8	32	58	87	To gen. meas. $Q(\beta)$
14	C64	19350	3660	20250	4480	19630	4910	1.22	1.28	0.75	−35	6.60	−68	−17.00	29	H	5.00	21	49	2.5	26	55	103	To gen. meas. $Q(\beta)$

APPENDIX 3

Spreadsheet Analysis of Field Measurements for Various Nordtank 150 kW Turbines at Langeland

Test locn	Chart ref.	Tx grid E	Tx grid N	W T grid E	W T grid N	Rx grid E	Rx grid N	Dist.T-W (km)	Dist.T-R (km)	Dist.W-R (km)	α (deg)	$P(\alpha)$ (dB)	β (deg)	$Q(\beta)$ (dB)	Chan	Pol.	$p-p$ max 2% divs	cycles in 10 s	F strength (dbμV/m)	Diffraction loss (dB)	S/I max (dB)	$K(\theta)$ (dB)	θ (degrees)	Comments
8-W6	C40	19350	3660	20220	4040	20470	4120	0.95	1.21	0.26	20	1.08	5	0.06	29	V	2.10	19			34	49	25	
8-W6	C41	19350	3660	20220	4040	20470	4120	0.95	1.21	0.26	20	2.05	5	0.11	29	H	1.60	19			37	53	25	
8-W7	C40	19350	3660	20230	4160	20470	4120	1.01	1.21	0.24	20	1.08	32	2.82	29	V	2.10	19			34	47	52	
8-W7	C41	19350	3660	20230	4160	20470	4120	1.01	1.21	0.24	20	2.05	32	5.37	29	H	1.60	19			37	48	52	
11-W4	C57	19350	3660	19600	4040	20220	4750	0.45	1.39	0.94	−9	0.42	3	0.03	29	H	1.70	19	78		36	47	7	
12-W4	C59	19350	3660	19600	4040	20120	4790	0.45	1.37	0.91	−13	0.91	0	0.00	29	H	1.60	20	75		36	48	13	
13-W4	C61	19350	3660	19600	4040	19950	4850	0.45	1.33	0.88	−21	2.25	−3	0.06	29	H	1.70	20	78	3.8	36	53	24	
14-W4	C63	19350	3660	19600	4040	19630	4910	0.45	1.28	0.87	−35	6.60	−11	0.57	29	H	2.00	21	66	2.5	34	53	46	
11-W5	C57	19350	3660	19660	4220	20220	4750	0.64	1.39	0.77	−9	0.42	8	0.32	29	H	1.70	19	78		36	45	1	
12-W5	C59	19350	3660	19660	4220	20120	4790	0.64	1.37	0.73	−13	0.91	5	0.11	29	H	1.60	20	75		36	47	9	
13-W5	C61	19350	3660	19660	4220	19950	4850	0.64	1.33	0.69	−21	2.25	−2	0.02	29	H	1.70	20	78	3.8	36	52	23	
14-W5	C63	19350	3660	19660	4220	19630	4910	0.64	1.28	0.69	−35	6.60	−15	1.16	29	H	2.00	21	66	2.5	34	51	50	
15-W2	C65	19350	3660	19720	2830	19490	2620	0.91	1.05	0.31	16	1.36	−305	18.57	29	H	0.40	21	81		48	42	72	
15-W2	C66	19350	3660	19720	2830	19490	2620	0.91	1.05	0.31	16	0.72	−305	9.77	29	V	0.20	21	81		54	57	72	
15-W2	C67	19350	3660	19720	2830	19490	2620	0.91	1.05	0.31	16	1.36	−305	−18.57	29	H	0.20	21			54	85	72	Toward turbine
16-W2	C68	19350	3660	19720	2830	20310	2120	0.91	1.81	0.92	−8	0.32	−8	0.31	29	H	1.50	14	74		38	44	16	
17-W2	C70	19350	3660	19720	2830	20320	1660	0.91	2.22	1.31	−2	0.02	−1	0.01	29	H	2.50	10	64	9	34	48	3	T-R not LOS
17-W2	C71	19350	3660	19720	2830	20320	1660	0.91	2.22	1.31	−2	0.01	−1	0.00	29	V	2.60	8	62	9	34	48	3	T-R not LOS
17-W2	C72	19350	3660	19720	2830	20320	1660	0.91	2.22	1.31	−2	0.01	−1	0.00	38	V	2.00	12	59	13	36	54	3	T-R not LOS
17-W2	C73	19350	3660	19720	2830	20320	1660	0.91	2.22	1.31	−2	0.02	−1	0.01	38	H	1.70	10	61	13	37	55	3	T-R not LOS
17-W2	C74	19350	3660	19720	2830	20320	1660	0.91	2.22	1.31	−2	0.02	−1	0.01	59	H	2.70	10	59	16	33	55	3	T-R not LOS
17-W2	C75	19350	3660	19720	2830	20320	1660	0.91	2.22	1.31	−2	0.01	−1	0.00	59	V	5.00	9	54	16	27	49	3	T-R not LOS
15-W3	C65	19350	3660	19280	3220	19490	2620	0.45	1.05	0.64	343	1.42	−12	0.68	29	H	0.40	21	81		48	60	28	
15-W3	C66	19350	3660	19280	3220	19490	2620	0.45	1.05	0.64	343	0.75	−12	0.36	29	V	0.20	21	81		54	66	28	
15-W3	C67	19350	3660	19280	3220	19490	2620	0.45	1.05	0.64	343	1.42	−12	−0.68	29	H	0.20	21			54	68	28	Toward turbine
16-W3	C68	19350	3660	19280	3220	20310	2120	0.45	1.81	1.51	319	9.28	−11	0.63	29	H	1.50	14	74		38	55	52	
17-W3	C70	19350	3660	19280	3220	20320	1660	0.45	2.22	1.87	325	6.55	−8	0.31	29	H	2.50	10	64	9	34	58	43	T-R not LOS
17-W3	C71	19350	3660	19280	3220	20320	1660	0.45	2.22	1.87	325	3.45	−8	0.16	29	V	2.60	8	62	9	34	55	43	T-R not LOS
17-W3	C72	19350	3660	19280	3220	20320	1660	0.45	2.22	1.87	325	3.45	−8	0.16	38	V	2.00	12	59	13	36	60	43	T-R not LOS
17-W3	C73	19350	3660	19280	3220	20320	1660	0.45	2.22	1.87	325	6.55	−8	0.31	38	H	1.70	10	61	13	37	65	43	T-R not LOS
17-W3	C74	19350	3660	19280	3220	20320	1660	0.45	2.22	1.87	325	6.55	−8	0.31	59	H	2.70	10	59	16	33	64	43	T-R not LOS
17-W3	C75	19350	3660	19280	3220	20320	1660	0.45	2.22	1.87	325	3.45	−8	0.16	59	V	5.00	9	54	16	27	55	43	T-R not LOS

APPENDIX 4

Spreadsheet Analysis of Field Measurements for Two Nordtank 300 kW Turbines in Jutland

Test locn	Chart ref.	Tx grid E	Tx grid N	W T grid E	W T grid N	Rx grid E	Rx grid N	Dist.T-W (km)	Dist.T-R (km)	Dist.W-R (km)	α (deg)	$P(\alpha)$ (dB)	β (deg)	$Q(\beta)$ (dB)	Chan	Pol.	p–p max 2% divs	cycles in 10 s	F strength (dbμV/m)	Diffraction loss (dB)	S/I max (dB)	$K(\theta)$ (dB)	θ (degrees)	Comments
N1-W1	C76	40160	29280	38430	30520	37510	31170	2.13	3.25	1.13	0	0.00	0	0.00	29	H	1.30	17	70.1		39	42	0	
N1-W1	C77	40160	29280	38430	30520	37510	31170	2.13	3.25	1.13	0	0.00	0	0.00	29	V	1.30	17	69.5		38	41	0	
N1-W1	C78	40160	29280	38430	30520	37510	31170	2.13	3.25	1.13	0	0.00	0	0.00	38	V	0.80	17	71.3		43	46	0	
N1-W1	C79	40160	29280	38430	30520	37510	31170	2.13	3.25	1.13	0	0.00	0	0.00	38	H	0.80	17	72.1		43	46	0	
N1-W1	C80	40160	29280	38430	30520	37510	31170	2.13	3.25	1.13	0	0.00	0	0.00	59	H	1.20	17	73.3		40	43	0	
N1-W1	C81	40160	29280	38430	30520	37510	31170	2.13	3.25	1.13	0	0.00	0	0.00	59	V	0.80	17	73.3		43	46	0	
N1-W2	C76	40160	29280	38800	31020	37510	31170	2.21	3.25	1.30	−16	1.39	−29	4.38	29	H	1.30	17	70.1		39	37	45	
N1-W2	C77	40160	29280	38800	31020	37510	31170	2.21	3.25	1.30	−16	0.73	−29	2.30	29	V	1.30	17	69.5		38	38	45	
N1-W2	C78	40160	29280	38800	31020	37510	31170	2.21	3.25	1.30	−16	0.73	−29	2.30	38	V	0.80	17	71.3		43	43	45	
N1-W2	C79	40160	29280	38800	31020	37510	31170	2.21	3.25	1.30	−16	1.39	−29	4.38	38	H	0.80	17	72.1		43	41	45	
N1-W2	C80	40160	29280	38800	31020	37510	31170	2.21	3.25	1.30	−16	1.39	−29	4.38	59	H	1.20	17	73.3		40	38	45	
N1-W2	C81	40160	29280	38800	31020	37510	31170	2.21	3.25	1.30	−16	0.73	−29	2.30	59	V	0.80	17	73.3		43	43	45	
N2	C82	38470	30600	38800	31020	39160	31490	0.53	1.13	0.59	0	0.00	0	0.00	29	V	3.50	1.2	84.2		31	42	1	
N2	C83	38470	30600	38800	31020	39160	31490	0.53	1.13	0.59	0	0.00	0	0.00	29	H	3.80	1.4	85		31	42	1	
N2	C84	38470	30600	38800	31020	39160	31490	0.53	1.13	0.59	0	0.00	0	0.00	38	H	7.50	1.25	83.4		25	36	1	
N2	C85	38470	30600	38800	31020	39160	31490	0.53	1.13	0.59	0	0.00	0	0.00	38	V	4.20	2.1	82.4		30	41	1	
N2	C86	38470	30600	38800	31020	39160	31490	0.53	1.13	0.59	0	0.00	0	0.00	59	V	10.50	2.5	77.3		22	33	1	
N2	C87	38470	30600	38800	31020	39160	31490	0.53	1.13	0.59	0	0.00	0	0.00	59	H	16.50	3.4	75		19	30	1	
N2	C88	38470	30600	38800	31020	39160	31490	0.53	1.13	0.59	0	0.00	0	0.00	59	H	11.80	10	75		21	32	1	
N2	C89	38470	30600	38800	31020	39160	31490	0.53	1.13	0.59	0	0.00	0	0.00	59	H	2.80	6.7	75		34	45	1	
N2	C90	38470	30600	38800	31020	39160	31490	0.53	1.13	0.59	0	0.00	0	0.00	59	H	11.00	11	75		22	33	1	
N3	C93	38470	30600	38800	31020	39150	31540	0.53	1.16	0.63	− 2	0.03	− 2	0.02	29	H	2.00	16	82.5		35	46	4	
N3	C94	38470	30600	38800	31020	39150	31540	0.53	1.16	0.63	− 2	0.01	− 2	0.01	29	V	1.90	13	80.5		36	47	4	
N3	C95	38470	30600	38800	31020	39150	31540	0.53	1.16	0.63	− 2	0.01	− 2	0.01	38	V	6.80	13	81.5		25	36	4	
N3	C96	38470	30600	38800	31020	39150	31540	0.53	1.16	0.63	− 2	0.03	− 2	0.02	38	H	5.50	13	81		27	38	4	
N3	C97	38470	30600	38800	31020	39150	31540	0.53	1.16	0.63	− 2	0.03	− 2	0.02	59	H	4.40	13	76.9		29	39	4	
N3	C98	38470	30600	38800	31020	39150	31540	0.53	1.16	0.63	− 2	0.01	− 2	0.01	59	V	4.50	13	77.3		28	39	4	
N4	C99	38470	30600	38800	31020	39200	31400	0.53	1.08	0.55	4	0.05	4	0.04	29	V	1.80	14	84.3		36	47	8	
N4	C100	38470	30600	38800	31020	39200	31400	0.53	1.08	0.55	4	0.09	4	0.08	29	H	2.10	14	84.3		36	48	8	
N4	C101	38470	30600	38800	31020	39200	31400	0.53	1.08	0.55	4	0.09	4	0.08	38	H	2.60	15	83		33	45	8	
N4	C102	38470	30600	38800	31020	39200	31400	0.53	1.08	0.55	4	0.05	4	0.04	38	V	2.10	15	84.3		36	47	8	
N4	C103	38470	30600	38800	31020	39200	31400	0.53	1.08	0.55	4	0.05	4	0.04	59	V	2.80	14	78.4		31	42	8	
N4	C104	38470	30600	38800	31020	39200	31400	0.53	1.08	0.55	4	0.09	4	0.08	59	H	9.00	15	77.1		24	35	8	
N5	C105	38470	30600	38800	31020	39270	31310	0.53	1.07	0.55	10	0.53	10	0.50	29	H	0.80	14			44	55	20	Close to Vestas
N5	C106	38470	30600	38800	31020	39270	31310	0.53	1.07	0.55	10	0.28	10	0.26	29	V	1.00	14			42	53	20	Close to Vestas
N5	C107	38470	30600	38800	31020	39270	31310	0.53	1.07	0.55	10	0.28	10	0.26	29	V	1.00	8			42	53	20	Close to Vestas
N5	C108	38470	30600	38800	31020	39270	31310	0.53	1.07	0.55	10	0.53	10	0.50	29	H	1.40	8			41	52	20	Close to Vestas
N5	C109	38470	30600	39350	31250	39270	31310	1.09	1.07	0.10	10	0.53	−102	−25.00	29	H	5.00	13			27	73	91	Toward Vestas
N6	C110	38470	30600	38800	31020	39380	31870	0.53	1.56	1.03	− 3	0.03	− 1	0.01	29	H	2.40	11			34	43	4	Trees obstructing
N6	C111	38470	30600	38800	31020	39380	31870	0.53	1.56	1.03	− 3	0.02	− 1	0.00	29	V	2.70	11			33	42	4	Trees obstructing

Appendix 4 *(cont.)*

Test locn	Chart ref.	Tx grid E	Tx grid N	W T grid E	W T grid N	Rx grid E	Rx grid N	Dist.T-W (km)	Dist.T-R (km)	Dist.W-R (km)	α (deg)	$P(\alpha)$ (dB)	β (deg)	$Q(\beta)$ (dB)	Chan	Pol.	p–p max 2% divs	cycles in 10 s	F strength (dbμV/m)	Diffraction loss (dB)	S/I max (dB)	$K(\theta)$ (dB)	θ (degrees)	Comments
N7	C112	38470	30600	38800	31020	39390	31760	0.53	1.48	0.95	0	0.00	0	0.00	38	V	4.50	9	78		29	39	0	
N7	C113	38470	30600	38800	31020	39390	31760	0.53	1.48	0.95	0	0.00	0	0.00	38	H	3.90	9	79		31	41	0	
N7	C114	38470	30600	38800	31020	39390	31760	0.53	1.48	0.95	0	0.00	0	0.00	29	H	4.70	9	78		28	38	0	
N7	C115	38470	30600	38800	31020	39390	31760	0.53	1.48	0.95	0	0.00	0	0.00	29	V	4.30	9	76		30	39	0	
N7	C116	38470	30600	38800	31020	39390	31760	0.53	1.48	0.95	0	0.00	0	0.00	59	V	30.50	9	66	9	12	30	0	Trees affect ch 59
N7	C117	38470	30600	38800	31020	39390	31760	0.53	1.48	0.95	0	0.00	0	0.00	59	H	18.00	9	68	8	17	34	0	Trees affect ch 59
N8	C118	38470	30600	38800	31020	39390	31820	0.53	1.53	0.99	−1	0.00	−1	0.00	29	V	0.70	9	77.4		45	54	2	
N8	C119	38470	30600	38800	31020	39390	31820	0.53	1.53	0.99	−1	0.01	−1	0.00	29	H	0.60	9	78.1		47	57	2	
N8	C120	38470	30600	38800	31020	39390	31820	0.53	1.53	0.99	−1	0.01	−1	0.00	38	H	2.70	9.5	80		33	42	2	
N8	C121	38470	30600	38800	31020	39390	31820	0.53	1.53	0.99	−1	0.00	−1	0.00	38	V	2.00	9	78.8		34	44	2	
N8	C122	38470	30600	38800	31020	39390	31820	0.53	1.53	0.99	−1	0.00	−1	0.00	59	V	10.70	10.5	75.7		21	31	2	
N8	C123	38470	30600	38800	31020	39390	31820	0.53	1.53	0.99	−1	0.01	−1	0.00	59	H	8.30	11.5	76		22	32	2	
N9	C124	38470	30600	38800	31020	39740	32040	0.53	1.92	1.39	3	0.05	1	0.01	29	H	0.80	14	74.3		44	52	5	
N9	C125	38470	30600	38800	31020	39740	32040	0.53	1.92	1.39	3	0.03	1	0.00	29	V	1.70	14	73.9		37	45	5	
N9	C126	38470	30600	38800	31020	39740	32040	0.53	1.92	1.39	3	0.03	1	0.00	38	V	2.50	14.5	72		33	42	5	
N9	C127	38470	30600	38800	31020	39740	32040	0.53	1.92	1.39	3	0.05	1	0.01	38	H	1.90	15	73.4		36	44	5	
N9	C128	38470	30600	38800	31020	39740	32040	0.53	1.92	1.39	3	0.05	1	0.01	59	H	3.50	15	72.5		31	39	5	
N9	C129	38470	30600	38800	31020	39740	32040	0.53	1.92	1.39	3	0.03	1	0.00	59	V	3.20	15	71.7		31	39	5	
N10	C130	38470	30600	38800	31020	41080	33820	0.53	4.14	3.61	1	0.00	0	0.00	29	V	3.70	16	63.7		29	35	1	
N11	C131	38470	30600	38800	31020	40880	33700	0.53	3.93	3.39	0	0.00	0	0.00	29	V	6.20	13	59.1		26	32	0	
N11	C132	38470	30600	38800	31020	40880	33700	0.53	3.93	3.39	0	0.00	0	0.00	29	H	6.40	13	61		25	32	0	
N11	C133	38470	30600	38800	31020	40880	33700	0.53	3.93	3.39	0	0.00	0	0.00	38	H	3.10	13.5	62.6		31	38	0	
N11	C134	38470	30600	38800	31020	40880	33700	0.53	3.93	3.39	0	0.00	0	0.00	38	V	6.20	13.3	62.3		24	31	0	
N11	C135	38470	30600	38800	31020	40880	33700	0.53	3.93	3.39	0	0.00	0	0.00	59	V	8.50	13.5	61.5		23	29	0	
N11	C136	38470	30600	38800	31020	40880	33700	0.53	3.93	3.39	0	0.00	0	0.00	59	H	5.40	12	62.2		27	34	0	
N12	C137	38470	30600	38800	31020	40400	33160	0.53	3.21	2.67	−1	0.01	0	0.00	59	H	5.50	10.5	68.7		27	34	1	
N12	C138	38470	30600	38800	31020	40400	33160	0.53	3.21	2.67	−1	0.00	0	0.00	59	V	5.00	10	67.7		27	34	1	
N12	C139	38470	30600	38800	31020	40400	33160	0.53	3.21	2.67	−1	0.00	0	0.00	38	V	6.50	10	68.4		25	32	1	
N12	C140	38470	30600	38800	31020	40400	33160	0.53	3.21	2.67	−1	0.01	0	0.00	38	H	3.40	10	68.7		31	38	1	
N12	C141	38470	30600	38800	31020	40400	33160	0.53	3.21	2.67	−1	0.01	0	0.00	29	H	3.20	10.5	68.5		31	38	1	
N12	C142	38470	30600	38800	31020	40400	33160	0.53	3.21	2.67	−1	0.00	0	0.00	29	V	3.50	11	67.3		30	37	1	
N13	C144	38470	30600	38800	31020	40730	32170	0.53	2.75	2.25	17	0.78	4	0.04	29	V	3.10	10	70.5		32	40	21	
N13	C145	38470	30600	38800	31020	40730	32170	0.53	2.75	2.25	17	1.48	4	0.08	29	H	1.90	11.5	71.5		36	45	21	
N13	C146	38470	30600	38800	31020	40730	32170	0.53	2.75	2.25	17	1.48	4	0.08	38	H	1.60	10	71.4		38	46	21	
N13	C147	38470	30600	38800	31020	40730	32170	0.53	2.75	2.25	17	0.78	4	0.04	38	V	2.70	10	70.6		33	41	21	
N13	C148	38470	30600	38800	31020	40730	32170	0.53	2.75	2.25	17	0.78	4	0.04	59	V	1.80	10	72.3		37	45	21	
N13	C149	38470	30600	38800	31020	40730	32170	0.53	2.75	2.25	17	1.48	4	0.08	59	H	0.80	10.5	72.2		44	52	21	
N13	C150	38470	30600	38800	31020	40730	32170	0.53	2.75	2.25	17	1.48	4	0.08	29	H	1.50	8.5	71.5		38	47	21	